Forecasting future range shifts of Xylella fastidiosa under climate change

Martin Godefroid, Astrid Cruaud, Jean-Claude Streito, Jean-Yves Rasplus, Jean-Pierre Rossi

Received: 7 June 2022 | Accepted: 17 August 2022

DOI: 10.1111/ppa.13637

Plant Pathology WILEY

ORIGINAL ARTICLE

Forecasting future range shifts of *Xylella fastidiosa* under climate change

Martin Godefroid[1,2] | Astrid Cruaud[1] | Jean-Claude Streito[1] | Jean-Yves Rasplus[1] | Jean-Pierre Rossi[1]

[1]CBGP, INRAE, CIRAD, IRD, Montpellier, France

[2]Department of Biogeography and Global Change, Museo Nacional de Ciencias Naturales (CSIC), Madrid, Spain

Correspondence
Martin Godefroid, Department of Biogeography and Global Change, Museo Nacional de Ciencias Naturales (CSIC), Madrid, Spain.
Email: martin.godefroid@gmail.com

Funding information
European Union Horizon 2020 research and innovation program, Grant/Award Number: 727987; French National Research Institute for Agriculture, Food and the Environment

Abstract

Xylella fastidiosa (Xf) is a vector-borne plant bacterium native to the Americas, which causes severe diseases to agricultural crops, ornamental plants and forest trees. The bacterium is becoming a source of worldwide health plant concern and disease outbreaks associated with Xf have occurred outside of its native range (in Europe, Asia and the Middle East). Several studies have estimated risks associated with Xf outbreaks in invaded regions under current climate conditions, but future climate change has been seldom addressed. In the present study, we calibrated correlative models of bioclimatic species distribution to forecast the potential range and severity of two economically important Xf-related diseases (Pierce's disease and the bacterial leaf scorch of shade trees) by the period 2040–2060. Models predict that conditions could become highly favourable for Pierce's disease in economically important wine-producing regions of the world, highlighting the need to design control strategies. Similarly, models suggest that risk of bacterial leaf scorch of shade trees might increase in temperate regions where it is still apparently absent. However, we note that substantial uncertainty in predictions arises from high levels of correlation among climatic variables in the calibration data set. The inherent lack of knowledge concerning whether the distribution of Xf-related diseases is at climatic equilibrium or not in Europe may also influence our predictions. The models provide valuable information to identify regions where increased surveillance efforts should be made and where control strategies are required.

KEYWORDS
bacterial leaf scorch of shade trees, invasion risk assessment, *Philaenus spumarius*, Pierce's disease of grapevine, species distribution modelling

1 | INTRODUCTION

The bacterium *Xylella fastidiosa* (Xf) (Wells et al., 1987) is an insect-borne plant pathogen native to the Americas, which invaded Europe, the Middle East and Asia (Bragard et al., 2019). The pathogen is responsible for socio-economically important plant diseases such as Pierce's disease of grapevine (PD), olive quick decline syndrome (OQDS), bacterial leaf scorch of shade trees (BLS), phony peach disease (PPD), citrus variegated chlorosis (CVC) and almond leaf scorch (ALS) (Bragard et al., 2019). Xf develops in plant xylem, obstructing

vessels and leading to water transport disruption, ultimately resulting in the death of plants when infection is severe. Not only in its native range (Tumber et al., 2014) but also in invaded regions (Saponari et al., 2019; Schneider et al., 2020), the economic impact of Xf-related plant diseases is huge, making the pathogen one of the biggest threats for worldwide agriculture.

The bacterium comprises six described subspecies, namely subsp. *fastidiosa*, subsp. *multiplex*, subsp. *pauca*, subsp. *taschke*, subsp. *sandyi* and subsp. *morus*, which differ in geographical origin, current spatial distribution and host-plant ranges (Nunney et al., 2013). In Europe, the first economically relevant Xf-related outbreak occurred in 2013 in the olive groves of Apulia in Italy, causing an unprecedented socio-economic disaster (Saponari et al., 2019). Afterwards, other outbreaks have occurred in France, Israel, Spain and Portugal on a diverse range of agricultural and ornamental plants (European Food Safety Authority Plant Health [EFSA PLH] Panel, Vos, et al., 2019b). Three Xf subspecies have been found to occur in Europe (*fastidiosa*, *multiplex*, *pauca*) sparking a considerable interest in assessing their potential geographical distribution (Bosso et al., 2016; EFSA PLH Panel, Bragard, et al., 2019a; Romero Fernández, 2020; Godefroid et al., 2019; Schneider et al., 2020) as well as in understanding drivers shaping the range of the main vectors of Xf in Europe (Godefroid et al., 2021; Godefroid & Durán, 2022). Studies attempting to predict the impact of global change on the future potential range and severity of Xf are, however, rare and consider neither full geographical information available for the pathogen nor putative differences among the different Xf subspecies (Bosso et al., 2016; Schneider et al., 2020).

Given its huge potential impact, a better understanding of the future geographical distribution and impact of Xf is needed to set up early-warning systems, improve surveillance, plan research programmes and design control strategies. Bioclimatic species distribution models (SDMs) are powerful tools to investigate the response of species to climate and predict the range of invasive species or distribution shifts induced by climate change (Peterson et al., 2011). SDMs are approaches that establish a statistical relationship between occurrence of a species and environmental covariates (Peterson et al., 2011). In the present survey, we aimed to predict the future climate suitability for PD and BLS at a worldwide scale.

2 | MATERIALS AND METHODS

2.1 | Distribution data

We used the Xf occurrence records provided by Godefroid et al. (2019). In addition, we collected new records available in recently published literature. Records were individually checked for accuracy, and unreliable records (e.g., too imprecise geographical situation) were discarded from the occurrence database. For BLS, we fitted models using presence records associated with subsp. *multiplex*, regardless of the identity of the host plants (i.e., 884 occurrences). Four records relative to subsp. *multiplex* were discarded from the database because they might be associated with microclimate conditions, namely, three records in the surroundings of the Ontario Lake, Canada (Goodwin & Zhang, 1997) and one record in Gates Lake, British Columbia, Canada, situated in a mountain valley. These points appear as outliers in the climatic space, and we hypothesize that large-scale macroclimatic rasters might be unable to reflect those microclimatic conditions. For example, the Ontario Lake is well known to provide microclimatic conditions in its vicinity (such large bodies of waters induce a warming of winter temperature and a reduction of frost days in winter; Dobson et al., 2020). To avoid overestimation of winter temperature resistance, we preferred to discard these sites. For PD, we accounted for all records related to the subsp. *fastidiosa*, regardless of the identity of the host plants, and additionally generated "artificial" presences in south-eastern United States (Texas, Florida, Alabama, Georgia, Mississippi, South Carolina, etc.), which are considered to represent the traditional range of PD and where severity is the highest (Hopkins & Purcell, 2002). Three hundred artificial presence records were randomly generated at latitudes ranging from 25° to 33.5° (altitude <200 m a.s.l) and 100 records were randomly generated between 33.5° and 35° (altitude <300 m a.s.l.) using the R package 'biomod2' (Thuiller et al., 2020). Accounting for these additional presences in model calibration aims to mimic the decreasing south-to-north severity of PD in eastern United States (Hopkins & Purcell, 2002). While some occurrences of subsp. *fastidiosa* were associated with plants other than grapevine, we advocate that using all records is a conservative approach that minimizes underestimation of risk. The final data set of PD records comprised 746 occurrences. The presence records available for these diseases are mapped in Appendix S1. Before fitting models, we removed duplicated records by allowing only one occurrence per pixel of the bioclimatic raster.

2.2 | Selection of climatic descriptors

Temperature strongly affects multiplication and survival of Xf in plants (Feil & Purcell, 2001). According to in vitro experiments, temperatures ranging from 17 to 25°C are considered to represent the optimal range for Xf multiplication (Feil & Purcell, 2001). Survival of Xf in plants is also known to be strongly affected by winter temperatures as infected grapevines tend to recover when exposed to cold temperatures (Purcell, 1980). The direct impact of rainfall and air moisture on a xylem-inhabiting bacterium is, however, unclear and, moisture-related climatic covariates might impact the distribution of vectors (Godefroid et al., 2021), host susceptibility to disease or complex interactions between host plants and the bacterium. Given the challenge of disentangling how the different components of Xf epidemiology are impacted by moisture-related covariates, we modelled the distribution of Xf-related diseases using two temperature descriptors extracted from the CHELSA (climatologies at high resolution for the earth's land surface areas) database (Karger et al., 2017) at a resolution of

5 arc-minutes, which reflect historical average climatic trends for the period 1979–2013 (referred to as "current climate conditions" in the rest of the manuscript). These covariates are the mean temperature of the coldest quarter of the year (bio11) and the mean temperature of the warmest 8-month period of the year. These variables aim to reflect bacterial winter survival and multiplicative growth from spring to autumn, respectively. While this approach is conservative, we recognize that we might overestimate risk in regions where moisture conditions are not suitable for multiplication of the bacterium in xylem vessels and/or vectors or establishment of competent vectors. However, we attempted to minimize risk underestimation because Xf is a harmful plant pathogen. We are aware that levels of risk overestimation that are too high can also be detrimental (e.g., implementation of unnecessary costly and environment-unfriendly control methods, loss of confidence in modelling outputs, etc.). However, we suggest that the modelling outputs provided here could primarily serve at identifying regions that should be surveyed, application of effective control methods being a further step of management of this pathogen.

To predict potential future risk of Xf-related diseases, we used climate change simulations provided by the fifth Intergovernmental Panel on Climate Change (IPCC). We used predictions from three global circulation models (GCMs) available, that is, the Canadian Earth System Model version 2 (CanESM2; Arora et al., 2011), the Model for Interdisciplinary Research on Climate version 5 MIROC5 (Watanabe et al., 2011) and the HadGEM2-CC (Martin et al., 2011) to account for uncertainty associated with difference among GCMs. Two representative concentration pathways (RCPs), RCP4.5 and RCP8.5, which predict moderate and important future greenhouse gas emissions, respectively, were accounted for (Van Vuuren et al., 2011).

2.3 | Modelling approach

We used a generalized linear model (GLM—binomial family) approach to model the distribution of both Xf-related diseases (Guisan et al., 2002). We allowed only linear species-covariate relationships and no interactions between descriptors were accounted for in the models. We avoided complex machine-learning approaches, which might model complex and hard to interpret species–environment relationships (Merow et al., 2013). While we recognize that quadratic features are probably more appropriate for most species (Austin, 2007), there is a serious risk that the native range of Xf would not be informative enough to capture the upper end of a unimodal response curve of the bacterium to temperatures. Indeed, the bacterium Xf occurs in the warmest regions of its native range (e.g., both subspp. *fastidiosa* and *multiplex* occur in Florida, Arizona, California, United States) as well as in warm tropical regions of South America (e.g., subsp. *pauca* occurs in equatorial Brazil), which makes accurate capture of upper thermal limits of Xf challenging. For this reason, we adopted a conservative approach and only allowed linear features in models (Merow et al., 2013), even though we recognize this parameter selection might lead to overestimation of risk in the warmest geographical areas of the earth.

We discriminated presences from two pseudoabsence data sets: (1) one data set encompassing 10,000 pseudoabsences generated in North America at latitudes ranging from 25° to 50° for PD and latitudes ranging from 25° to 65° for BLS (referred to as models *BCK_NA* hereafter), and (2) one data set encompassing 20,000 pseudoabsences equally distributed in Europe and North America (models *BCK_NAEU*). For PD, pseudoabsences were generated in Europe at latitudes ranging from 35° to 50° (approximately the latitude range of grapevine cultivation in Europe) and at longitudes ranging from −10° to 40°. For BLS, pseudoabsences were generated in Europe at latitudes ranging from 35° to 72° and at longitudes ranging from −10° to 40° (Appendix S2). The pseudoabsences were randomly generated in these areas excluding pixels associated with an occurrence record of Xf. These pseudoabsences were generated using the R package 'biomod2' (Thuiller et al., 2020). Overall, according to this selection of pseudoabsences, the models *BCK_NA* do not make any assumption on climatic equilibrium of Xf-related plant diseases in Europe while the models *BCK_NAEU* assume that the spatial pattern of Xf-related plant diseases outbreaks in Europe partly reflect the climate preferences of the pathogen (because pseudoabsences are generated in Europe).

We used a cross-validation procedure to evaluate accuracy of models (Fielding & Bell, 1997). Presences and pseudoabsences were randomly split into a calibration data set (80% of data) and an evaluation data set (the remaining 20% of data). The predictive accuracy of models was assessed by calculating the area under the curve of the receiving operator curve (AUC; Fielding & Bell, 1997) and the true skill statistics (TSS; Allouche et al., 2006). This approach was repeated 10 times to account for the uncertainty arising from the cross-validation procedure. We produced maps depicting four classes of severity of the disease in infected plants using the following thresholds: extremely low, climatic suitability <0.25; low to moderate, climatic suitability ≥0.25 and <0.5; moderate to high, climatic suitability ≥0.5 and <0.75; severe, climatic suitability ≥0.75. To depict differences between calibration and projected climatic spaces, we calculated the multivariate environmental similarity surfaces (MESS) as described by Elith et al. (2010). The MESS calculation represents how similar a point in the projected area is to the set of calibration points, with respect to the set of predictor variables. The MESS index was calculated using the R package 'dismo' (Hijmans et al., 2017). The MESS maps aim to identify which geographical areas are climatically highly different from the calibration data (MESS index <0). We used the R package 'biomod2' to calibrate and evaluate the models (Thuiller et al., 2020). To assess the reliability of predictions, we also extracted the predicted climatic suitability at areas with current severe Xf-related outbreaks. For PD, we considered subsp. *fastidiosa*-related outbreaks in Balearic Islands (Majorca), Israel (Hua valley) and Taiwan. For BLS, we considered subsp. *multiplex*-related outbreaks in Portugal (Vila Nova de Gaia), Spain (Castell de Guadalest and Majorca), France (Ajaccio, Corsica and Nice, Provence-Alpes Côte d'Azur) and Italy (Grossetto,

Tuscany). To assess the climate change-induced shift in climatic suitability for PD in important wine-growing regions of the world, we built a nonexhaustive list of major wine-producing countries (France, Italy, Spain, Portugal, United States, China, Australia, South Africa, Argentina, Chile). Based on expert knowledge and literature, we made a list of the main wine-producing regions of these countries. We then extracted climate suitability estimation under current and future climate conditions for all of them.

3 | RESULTS

3.1 | Pierce's disease of grapevine

We found high differences among both sets of models regarding the relative importance of analysed variables. In the models *BCK_NA*, winter temperatures yielded the highest relative contribution (mean variable importance = 0.37, standard error = 0.06) while temperatures of the warmest 8-month period had a lower importance (mean variable importance = 0.31, standard error = 0.06). The modelled relationship curves between the probability of presence of PD and both covariates are available in Appendix S3a. In the models *BCK_NAEU*, winter temperatures had negligible importance (variable importance always inferior to 0.02). For the model *BCK_NAEU*, the modelled relationship curves between the probability of presence of PD and both covariates are available in Appendix S3b. We advocate that the models *BCK_NAEU* yield little reliable modelled response curves. Indeed, the high values of predicted climatic suitability at extremely low values of bio11 (Appendix S3b) are incongruent with available knowledge of biology of the bacterium and the well-documented cold curing phenomena (recovery of an infected plant when winter temperatures are low; Purcell, 1980). We believe that presenting a model where winter temperatures have no importance in the case of Xf is unrealistic according to the current knowledge of Xf physiology. For this reason, we discarded models *BCK_NAEU* for PD, and adopted a conservative approach by only presenting outputs and evaluation metrics relative to the model *BCK_NA* in the rest of the manuscript.

The models *BCK_NA* yielded good evaluation metrics (mean AUC = 0.84, standard error = 0.01; mean TSS = 0.65, standard error = 0.03). All recorded outbreaks induced by the subsp. *fastidiosa* in Europe and Asia (i.e., in Balearic islands, Israel and Taiwan) occurred in regions with high predicted climatic suitability ranging from 713.7 to 850.8, suggesting good predictive power of the model. The MESS maps suggest that tropical areas of South America, south-east Asia and Africa as well as extremely cold regions of the northern hemisphere in North America and Eurasia are climatically different from the calibration data set under current and future climate conditions (MESS values <0; Appendix S4a–c).

For Europe, the models predict that only a few parts of the Mediterranean area are moderately to highly suitable for PD under current climatic conditions (lowlands of Mediterranean islands, southern Spain and southern Italy [e.g., Apulia region], coastal regions of the Iberian and Italian Peninsula, south-eastern France, Greece and Turkey [Appendix S4d,e]). In other important wine-producing regions of the world, relatively moderate to high climatic suitability is predicted in southern California, coastal regions of South Africa and of south-western Australia (Appendices S4d,e and S5). Conversely, important wine-growing regions of Chile and Argentina are predicted as moderately to little suitable (Appendices S4d,e and S5). Most of the important wine-producing regions of China are predicted as little suitable (Appendix S5).

Under the two RCP scenarios considered here, models predict that the climatic suitability for PD will increase in most of Europe by the period 2040–2060 (Figure 1; Appendices S4f–h and S5). Noticeably, disease severity is predicted to become moderate to high in important wine-growing regions including France (e.g., Bordeaux, Corsica and Occitania), Italy (e.g., Latium, Apulia, Sardegna, Umbria, Sicily, Tuscany, Marche, Campania, Calabria), Portugal (e.g., Douro, Dão, Barraida, Alentejo), Spain (e.g., Castilla la Mancha, Priorat, Huelva, Jerez, Galicia, Balearic islands, Jumilla), South Africa, Australia (e.g., New South Wales, western and southern Australia), Chile and Argentina (e.g., Catamarca, Salta, Rio Negro) (Figure 1; Appendices S4f–h and S5). Under scenario RCP4.5, models predict a 10.9% and a 6.99% increase in the extent of areas classified as severe risk in northern and southern hemispheres, respectively. Under scenario RCP8.5, models predict a 13.09% and an 8.93% increase in the extent of areas classified as severe risk in the northern and southern hemispheres, respectively.

3.2 | Bacterial leaf scorch of shade trees

Both sets of models yielded good predictive accuracy metrics (*BCK_NA*: mean AUC = 0.85, standard error = 0.01; mean TSS = 0.68, standard error = 0.03; *BCK_NAEU*: mean AUC = 0.87, standard error = 0.01; mean TSS = 0.71, standard error = 0.03). In the models *BCK_NA*, winter temperatures had the highest relative contribution (mean variable importance = 0.98, standard error = 0.02) while temperatures of the warmest 8-month period had a negligible relative contribution (mean variable importance = 0.001, standard error = 0.002; Appendix S3c). In the models *BCK_NAEU*, both covariates had similar relative contribution (mean variable importance of bio11 = 0.33, standard error = 0.04; mean variable importance of the warmest 8-month period = 0.39, standard error = 0.04; Appendix S3d).

According to MESS maps, most of the world, except some tropical areas of South America, south-east Asia and Africa and extremely cold regions of the northern hemisphere in North America and Eurasia, are climatically different from the calibration data set under current and future climate conditions (MESS values <0; Appendices S5 and S6a–c).

For Europe, both sets of models predict many parts of the Mediterranean area as currently highly suitable for BLS under current climatic conditions including most of the lowlands of the Mediterranean basin (Appendices S5 and S6e). However, the sets

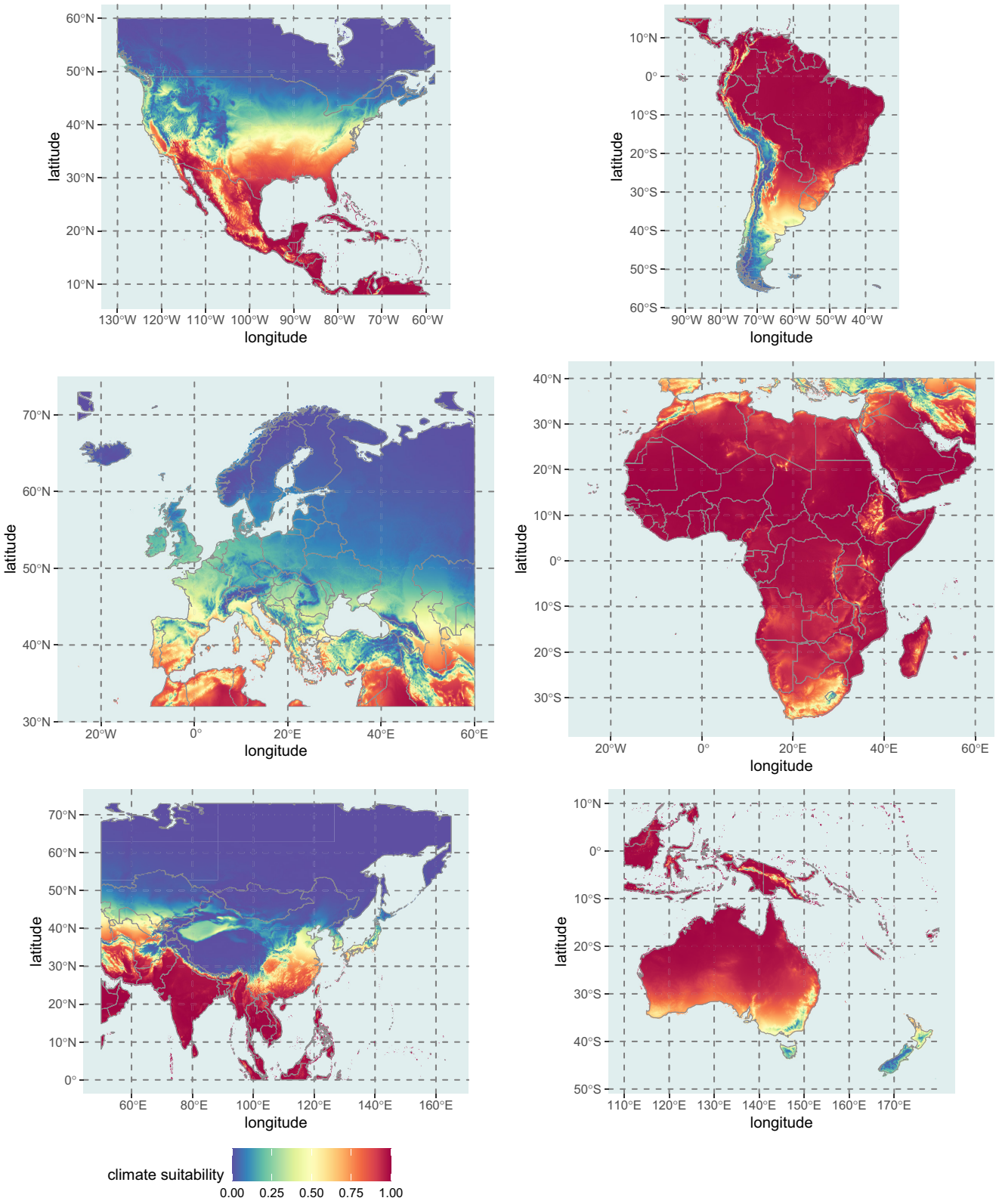

FIGURE 1 Climate suitability maps for Pierce's disease of grapevine provided by generalized linear models under future climate conditions (period 2040–2060). We mapped the average predicted climate suitability among three global climate models (MIROC5, CanESM2, HadGEM2-CC) simulating a scenario of moderate future greenhouse gas emissions (RCP4.5).

of models differ from each other in the predicted climatic suitability in northern Europe (i.e., Benelux, UK, northern France). Indeed, the model *BCK_NA* predicts high climatic suitability in these regions (Appendix S5d,e) unlike the model *BCK_NAEU* (Appendix S6d,e). Across the rest of the world, predicted climatic suitability is relatively high in tropical and temperate regions, excluding cold regions

of southern South America, northern North America, Eurasia (Russia, Scandinavia), and areas of high altitude (Appendices S5d,e and S6d,e). Regardless of the RCP scenario, models predict that the climatic suitability for BLS will increase in most temperate regions of the world and could threaten them, while the coldest regions of Eurasia, North and South America, and areas of high altitude will remain unsuitable (Figures 2 and 3; Appendices S5f–h and S6f–h). Under the scenario RCP4.5, models *BCK_NA* predict a 7.54% and a 2.86% increase in the extent of areas classified at severe risk in the northern and southern hemispheres, respectively. Under the scenario RCP8.5, these values are 9.37% and 3.82%, respectively. Under the scenario RCP4.5, models *BCK_NAEU* predict a 7.54% and a 2.86% increase in the extent of areas classified at severe risk in northern and southern hemispheres, respectively; under the scenario RCP8.5, these values are 11.88% and 4.83%, respectively. All recorded outbreaks induced by the Xf subsp. *multiplex* in Europe (in France, Portugal, Spain, Italy) occurred in regions with predicted climatic suitability ranging from 0.71 to 0.85.

4 | DISCUSSION

Xf outbreaks are currently restricted to a few regions of the world. This spatial pattern is shaped by climate tolerances of both the bacterium (Purcell, 1980) and competent vectors (Godefroid et al., 2021) as well as the history of plant trade (Almeida & Nunney, 2015; Moralejo et al., 2019; Nunney et al., 2013; Soubeyrand et al., 2018). Unsurprisingly, bioclimatic models suggest that temperatures during winter and vegetative growth of plants are important climatic factors shaping the distribution of Xf outbreaks. Therefore, models predict moderate to high climate suitability for both BLS and PD conditions in most of tropical and temperate regions of the world that are characterized by mild winter temperatures and relatively high temperature from spring to autumn (Appendix S3). Under current temperature conditions, the models predict high climate suitability in regions where subsp. *fastidiosa*-related outbreaks have recently occurred beyond its native range (e.g., in Taiwan, Balearic Islands, Israel). Similarly, areas of subsp. *multiplex*-related outbreaks were predicted by the models as highly climatically suitable for BLS, including Balearic Islands, lowlands in Corsica Island, coastal regions of south-eastern France, coastal Portugal, coastal parts of Tuscany. This suggests the models have an overall good predictive accuracy.

Some of the most important wine-producing regions worldwide, where severe PD outbreaks have not yet occurred, are predicted as moderately or little suitable for PD under current climate conditions; for example, wine-producing regions of France (Bordeaux, Occitania, Champagne, Alsace, Burgundy), lowlands in northern Italy, central and north Spain (Appendices S4 and S5). This finding might explain why no outbreak of PD has ever occurred in most of the European wine-producing areas, despite the presence of competent vectors (Godefroid et al., 2021) and massive importation of putatively Xf-infected grapevines from the United States after the phylloxera crisis in the 19th century. Strikingly, the present study suggests that climate suitability for PD will become high in some of the above-mentioned wine-producing regions (Figure 1; Appendices S4f–h and S5). Indeed, models predict that global change might induce a major increase of climatic suitability in most of wine-producing regions of the world. Our predictions suggest that the severity of PD might switch from low/moderate to high in some of the most economically important wine-growing regions of France (e.g., Bordeaux, Corsica and Occitania), Italy (e.g., Latium, Apulia, Sardegna, Umbria, Sicily, Tuscany, Marche, Campania, Calabria), Portugal (e.g., Douro, Dão, Barraida, Alentejo) and Spain (e.g., Castilla la Mancha, Priorat, Huelva, Jerez, Galicia, Balearic islands, Jumilla), as well as in most wine-producing areas of South Africa, Australia (e.g., in New South Wales, western and southern Australia), Chile and Argentina (e.g., Catamarca, Salta, Mendoza, Rio Negro) (Figure 1; Appendices S4f–h and S5). This highlights the need for the design of research programmes and control strategies to anticipate the impact of potential outbreaks. In China, one of the top producers of wine, severity of PD should remain low in most economically important grape-producing regions despite the ongoing increase of temperature (Appendix S5). Global change is also expected to induce a major increase of climate suitability for BLS in most temperate regions of the world that are not at high risk so far. Indeed, most temperate regions of western Europe, eastern Asia and the Americas, except very cold regions situated at extreme latitudes, might become at high risk for BLS outbreaks (Figures 2 and 3; Appendices S5 and S6). We believe that risk maps obtained here for PD are probably interesting proxies to estimate potential range/impact of the Xf subsp. *pauca*—mainly distributed in South America and responsible for the harmful OQDS and CVC. In the present study, we did not show modelling outputs specific for this subspecies although it is responsible for harmful outbreaks beyond its native range, for example, in Apulia, Italy (Saponari et al., 2019). The main reason for not considering subsp. *pauca* in the paper was the risk of incomplete sampling of subsp. *pauca* in its native range, South America, compared to North America, which could lead to problematic outputs.

Overall, climatic differences between the calibration data sets and most of the temperate regions where the models were projected are minor, which gives credibility to climate suitability estimations (positive MESS index). We acknowledge that uncertainty exists in some tropical areas of Africa, South America and south-east Asia, where temperatures are high all year (negative MESS index). Also, we recognize that omitting moisture-related covariates in our modelling effort might lead to overestimation of risk in some areas where moisture is not suitable for multiplication of the bacterium. Nevertheless, in our opinion, the largest source of uncertainty is the choice of the extent of the background area where pseudoabsences used for model fitting were generated (Lobo et al., 2010). Indeed, models calibrated only with pseudoabsences generated in the Americas (models *BCK_NA*) tend to convey a minor (or negligible) importance to temperature conditions occurring during plant vegetative growth (spring to autumn) for BLS (Appendix S3c). Conversely, models calibrated using pseudoabsences generated in both the Americas and Europe (models *BCK_NAEU*) tend to convey

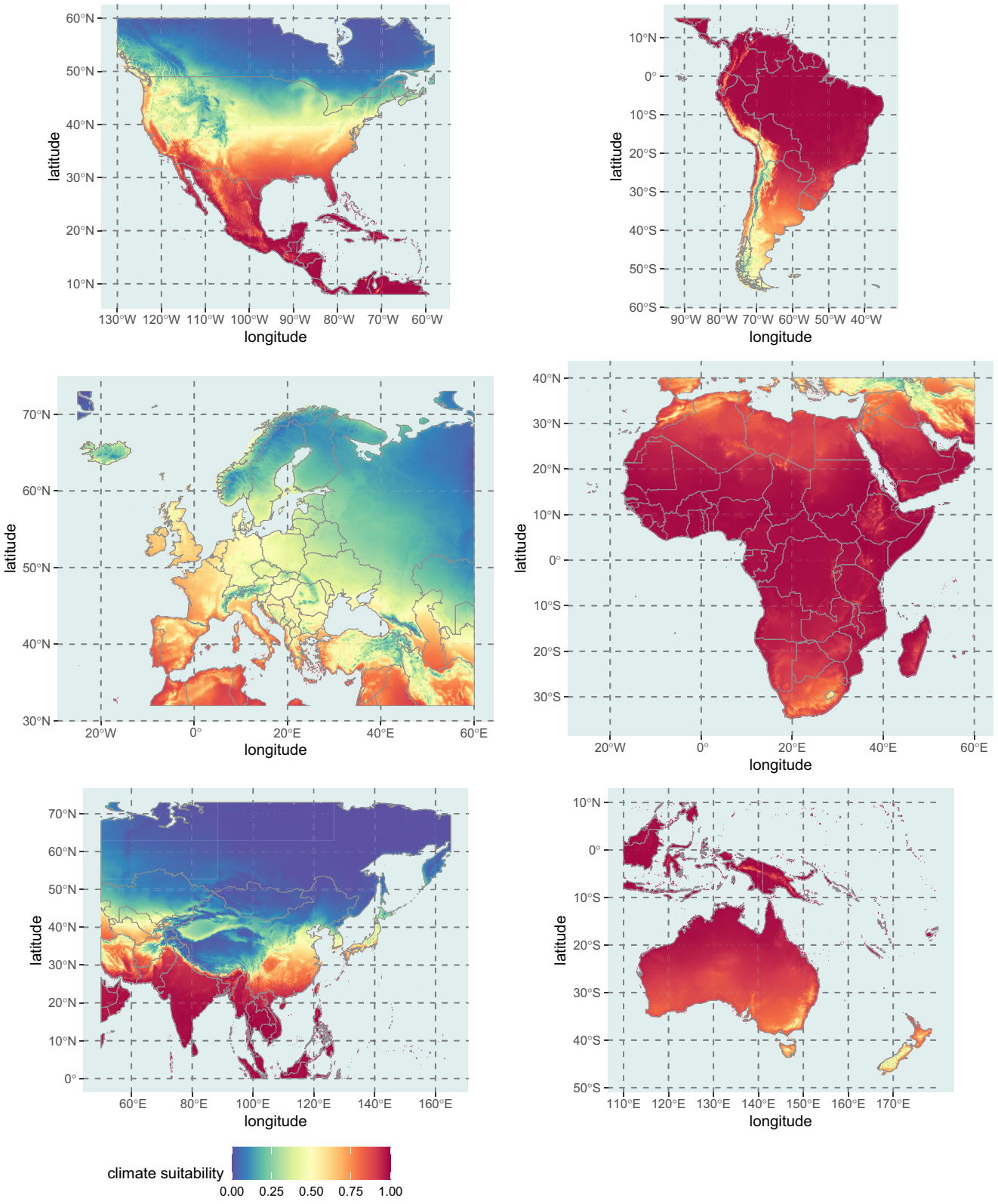

FIGURE 2 Climate suitability maps for bacterial leaf scorch of shade trees provided by generalized linear models under future climate conditions (period 2040–2060). We mapped the average predicted climate suitability among three global climate models (MIROC5, CanESM2, HadGEM2-CC) simulating a scenario of moderate future greenhouse gas emissions (RCP4.5). Models were fitted with pseudoabsences generated in North America (model *BCK_NA*).

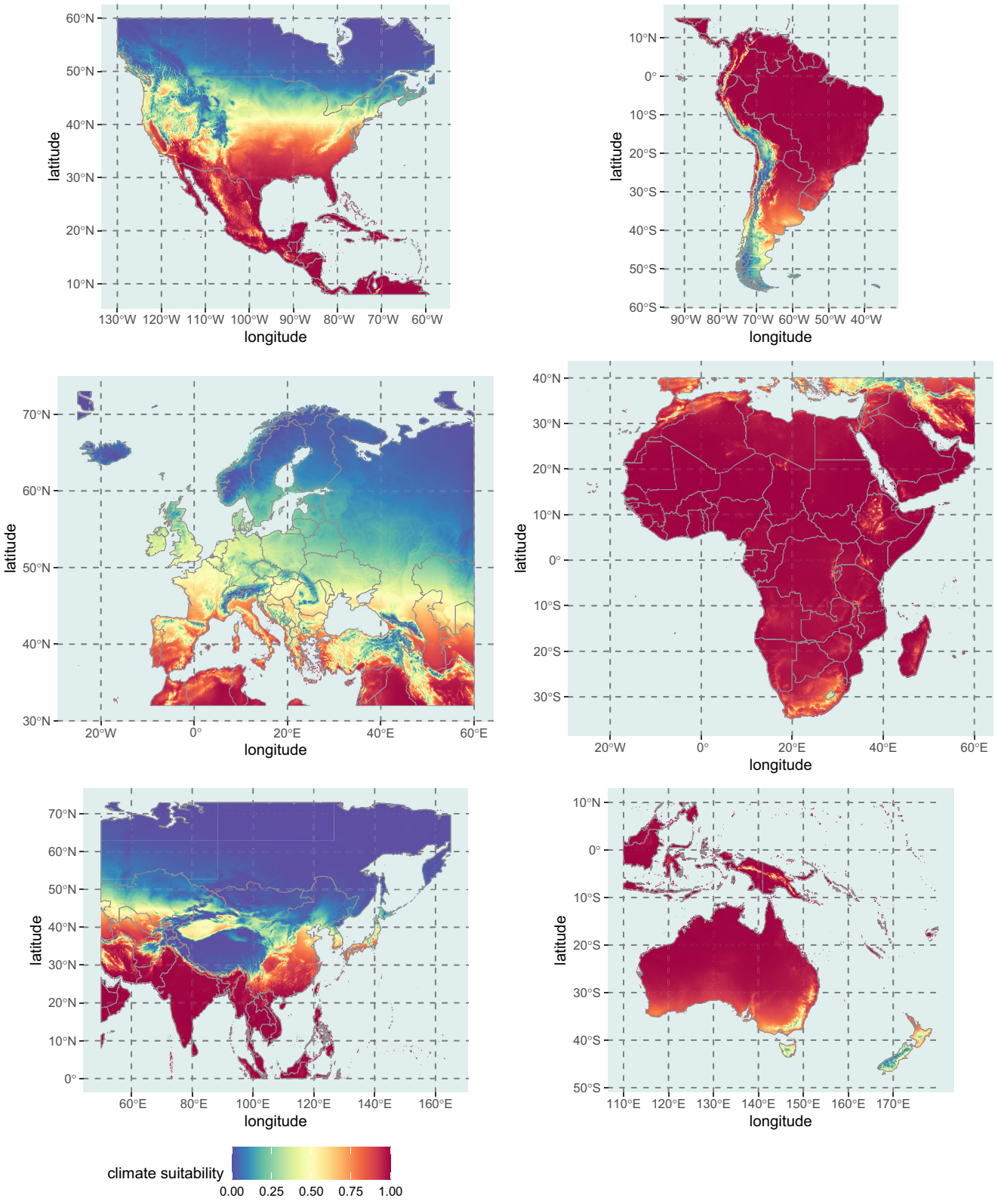

FIGURE 3 Climate suitability maps for bacterial leaf scorch of shade trees provided by generalized linear models under future climate conditions (period 2040–2060). We mapped the average predicted climate suitability among three global climate models (MIROC5, CanESM2, HadGEM2-CC) simulating a scenario of moderate future greenhouse gas emissions (RCP4.5). Models were fitted with pseudoabsences generated in North America and Europe (model *BCK_NAEU*).

higher relative importance to temperature occurring from spring to autumn for BLS (Appendix S3d). Therefore, models calibrated with absences generated only in the Americas (models *BCK_NA*) identify many northern regions of Europe as highly suitable for BLS (e.g., UK, Benelux, Scandinavia) unlike the *BCK_NAEU* models. This difference highlights how the outputs of models are dependent on the assumption of climatic equilibrium of Xf-related diseases in Europe. This is particularly true regarding the impact of temperatures during the warmest period of the year on Xf-related symptom expression. Apparently, no Xf-related disease outbreaks have ever occurred in these northern regions, and this pattern is presumably not due to the absence of vectors (Cruaud et al., 2018; Godefroid et al., 2021) or suitable hosts (e.g., oaks are widely distributed in northern Europe). Also, we could reasonably assume that Xf has been introduced into these regions as has probably occurred in many other parts of Europe (Moralejo et al., 2020; Soubeyrand et al., 2018), although this hypothesis is speculative. In such a context, this study highlights that climatic features other than winter temperatures, particularly the temperature during the vegetative growth of plants, might play a major role in shaping the spatial pattern of Xf-related outbreaks. This hypothesis is congruent with the finding that a temperature threshold is needed for multiplication of the bacterium in grapevines (Feil & Purcell, 2001). However, disentangling the role of both covariates (i.e., the winter and spring–autumn temperatures) is challenging with correlative approaches for a species if we do not know whether the invaded range is at equilibrium or not. Moreover, both covariates are highly correlated in the Americas, which precludes an easy discrimination of their respective roles in shaping the spatial distribution of the bacterium. Thus, although the present study highlights this source of uncertainty, further mechanistic models need to be performed to fill this gap in knowledge and reduce uncertainty in predictions.

The correlative models presented here provide a straightforward estimation of future shift in distribution of two Xf-related diseases. However, we want to draw attention to several weaknesses associated to correlative bioclimatic SDMs. One important pitfall comes from the fact that SDMs only depict the *realized* niche of species and do not account for geographical barriers, biotic interactions and dispersal limits (plant trade in the specific case of Xf), which contribute to shape the range of species (Jiménez-Valverde et al., 2008). Our models only focus on the presence of the bacterium in plants and do not account for the distribution of vectors, which also play a role in shaping the spatial pattern of Xf distribution (Godefroid et al., 2021). The maps presented here should ideally be included in more complex epidemiological models considering the local community of competent vectors and their transmission abilities. We also cannot reject the possibility of further genetic adaptation to new climate conditions. This potential adaptation cannot be anticipated in the correlative SDMs presented here. Finally, interactions between the different subspecies of Xf and their different host ranges may also be important drivers shaping the spatial occurrence of Xf-related outbreaks. Therefore, we suggest that such plant/pathogen interactions should be addressed in further modelling efforts.

This study provides important information for the design of future monitoring plans for two economically important Xf-related plant diseases: PD and BLS. Assessing the possible consequences of climate change upon potential distribution of pests and plant diseases is a key aspect of preventive crop protection (Reaser et al., 2020; Ricciardi et al., 2017). A special effort in detection and management, as well as possible amendment of policies for plant product exchange may need to be implemented in territories at risk. Surveillance based on plants and insects (Cruaud et al., 2018) should include not only areas where outbreaks occur, but also territories where climate suitability is favourable and where Xf-related outbreaks have apparently not yet occurred. In addition, special attention should be paid to regions that will shortly change to suitable conditions. Thus, the development of an efficient international cooperation with shared epidemiosurveillance systems and data is essential for the circulation of information among organizations in charge of management (Giovani et al., 2020).

ACKNOWLEDGEMENTS

This work was funded by the European Union Horizon 2020 research and innovation program under grant agreement no. 727987 XF-ACTORS and the Plant health department of the INRAE (French National Research Institute for Agriculture, Food and the Environment).

DATA AVAILABILITY STATEMENT

Data are available from the authors upon reasonable request.

ORCID

Martin Godefroid https://orcid.org/0000-0002-1887-9135

REFERENCES

Allouche, O., Tsoar, A. & Kadmon, R. (2006) Assessing the accuracy of species distribution models: prevalence, kappa and the true skill statistic (TSS). *Journal of Applied Ecology*, 43, 1223–1232.

Almeida, R.P.P. & Nunney, L. (2015) How do plant diseases caused by *Xylella fastidiosa* emerge? *Plant Disease*, 99, 1457–1467.

Arora, V.K., Scinocca, J.F., Boer, G.J., Christian, J.R., Denman, K.L., Flato, G.M. et al. (2011) Carbon emission limits required to satisfy future representative concentration pathways of greenhouse gases. *Geophysical Research Letters*, 38, L05805.

Austin, M. (2007) Species distribution models and ecological theory: a critical assessment and some possible new approaches. *Ecological Modelling*, 200, 1–19.

Bosso, L., Di Febbraro, M., Cristinzio, G., Zoina, A. & Russo, D. (2016) Shedding light on the effects of climate change on the potential distribution of *Xylella fastidiosa* in the Mediterranean basin. *Biological Invasions*, 18, 1759–1768.

Bragard, C., Dehnen-Schmutz, K., Di Serio, F., Gonthier, P., Jacques, M.-A., Miret, J.A.J. et al. (2019) Update of the Scientific Opinion on the risks to plant health posed by *Xylella fastidiosa* in the EU territory. *EFSA Journal*, 17, e05665.

Cruaud, A., Gonzalez, A.-A., Godefroid, M., Nidelet, S., Streito, J.-C., Thuillier, J.-M. et al. (2018) Using insects to detect, monitor and

predict the distribution of *Xylella fastidiosa*: a case study in Corsica. *Scientific Reports*, 8, 15628.
Dobson, K.C., Beaty, L.E., Rutter, M.A., Hed, B. & Campbell, M.A. (2020) The influence of Lake Erie on changes in temperature and frost dates. *International Journal of Climatology*, 40, 5590–5598.
Elith, J., Kearney, M. & Phillips, S. (2010) The art of modelling range-shifting species. *Methods in Ecology and Evolution*, 1, 330–342.
European Food Safety Authority Plant Health (EFSA PLH) Panel, Bragard, C., Dehnen-Schmutz, K., Di Serio, F., Gonthier, P., Jacques, M.-A. et al. (2019) Effectiveness of in planta control measures for *Xylella fastidiosa*. *EFSA Journal*, 17, e05666.
European Food Safety Authority Plant Health (EFSA PLH) Panel, Vos, S., Camilleri, M., Diakaki, M., Lazaro, E., Parnell, S. et al. (2019) Pest survey card on *Xylella fastidiosa*. *EFSA Supporting Publication*, 16, 1667E.
Feil, H. & Purcell, A.H. (2001) Temperature-dependent growth and survival of *Xylella fastidiosa* in vitro and in potted grapevines. *Plant Disease*, 85, 1230–1234.
Fielding, A.H. & Bell, J.F. (1997) A review of methods for the assessment of prediction errors in conservation presence/absence models. *Environmental Conservation*, 24, 38–49.
Giovani, B., Blümel, S., Lopian, R., Teulon, D., Bloem, S., Martinez, C.G. et al. (2020) Science diplomacy for plant health. *Nature Plants*, 6, 902–905.
Godefroid, M. & Durán, J.M. (2022) Composition of landscape impacts the distribution of the main vectors of *Xylella fastidiosa* in southern Spain. *Journal of Applied Entomology*, 146, 666–675.
Godefroid, M., Cruaud, A., Streito, J.-C., Rasplus, J.-Y. & Rossi, J.-P. (2019) *Xylella fastidiosa*: climate suitability of European continent. *Scientific Reports*, 9, 8844.
Godefroid, M., Morente, M., Schartel, T., Cornara, D., Purcell, A., Gallego, D. et al. (2021) Climate tolerances of *Philaenus spumarius* should be considered in risk assessment of disease outbreaks related to *Xylella fastidiosa*. *Journal of Pest Science*, 95, 855–868.
Goodwin, P.H. & Zhang, S. (1997) Distribution of *Xylella fastidiosa* in southern Ontario as determined by the polymerase chain reaction. *Canadian Journal of Plant Pathology*, 19, 13–18.
Guisan, A., Edwards, T.C., Jr. & Hastie, T. (2002) Generalized linear and generalized additive models in studies of species distributions: setting the scene. *Ecological Modelling*, 157, 89–100.
Hijmans, R.J., Phillips, S., Leathwick, J. & Elith, J. (2017) Package 'dismo'. *Circles*, 9, 1–68.
Hopkins, D.L. & Purcell, A.H. (2002) *Xylella fastidiosa*: cause of Pierce's disease of grapevine and other emergent diseases. *Plant Disease*, 86, 1056–1066.
Jiménez-Valverde, A., Lobo, J.M. & Hortal, J. (2008) Not as good as they seem: the importance of concepts in species distribution modelling. *Diversity and Distributions*, 14, 885–890.
Karger, D.N., Conrad, O., Böhner, J., Kawohl, T., Kreft, H., Soria-Auza, R.W. et al. (2017) Climatologies at high resolution for the Emajarth's land surface areas. *Scientific Data*, 4, 170122.
Lobo, J.M., Jiménez-Valverde, A. & Hortal, J. (2010) The uncertain nature of absences and their importance in species distribution modelling. *Ecography*, 33, 103–114.
Martin, G.M., Bellouin, N., Collins, W.J., Culverwell, I.D., Halloran, P.R., Hardiman, S.C. et al. (2011) The HadGEM2 family of Met Office unified model climate configurations. *Geoscientific Model Development*, 4, 723–757.
Merow, C., Smith, M.J. & Silander, J.A., Jr. (2013) A practical guide to MaxEnt for modeling species' distributions: what it does, and why inputs and settings matter. *Ecography*, 36, 1058–1069.
Moralejo, E., Borràs, D., Gomila, M., Montesinos, M., Adrover, F., Juan, A. et al. (2019) Insights into the epidemiology of Pierce's disease in vineyards of Mallorca, Spain. *Plant Pathology*, 68, 1458–1471.
Moralejo, E., Gomila, M., Montesinos, M., Borras, D., Pascual, A., Nieto, A. et al. (2020) Phylogenetic inference enables reconstruction of a long-overlooked outbreak of almond leaf scorch disease (*Xylella fastidiosa*) in Europe. *Communications Biology*, 3, 560.
Nunney, L., Vickerman, D.B., Bromley, R.E., Russell, S.A., Hartman, J.R., Morano, L.D. et al. (2013) Recent evolutionary radiation and host plant specialization in the *Xylella fastidiosa* subspecies native to the United States. *Applied and Environmental Microbiology*, 79, 2189–2200.
Peterson, A.T., Soberón, J., Pearson, R.G., Anderson, R.P., Martinez-Meyer, E., Nakamura, M. et al. (2011) *Ecological niches and geographic distributions (MPB-49)*. Princeton, USA: Princeton University Press.
Purcell, A.H. (1980) Environmental therapy for Pierce's disease of grapevines. *Plant Disease*, 64, 388–390.
Reaser JK, Burgiel SW, Kirkey J, Brantley KA, Veatch SD, Burgos-Rodriguez (2020) The early detection of and rapid response (EDRR) to invasive species: a conceptual framework and federal capacities assessment. *Biological Invasions*, 22, 1–19.
Ricciardi, A., Blackburn, T.M., Carlton, J.T., Dick, J.T.A., Hulme, P.E., Iacarella, J.C. et al. (2017) Invasion science: a horizon scan of emerging challenges and opportunities. *Trends in Ecology and Evolution*, 32, 464–474.
Romero Fernández, M.G. (2020) Análisis de distribución potencial de *Xylella fastidiosa* subsp. *multiplex* ST-6 y *Philaenus spumarius* en el sur de la Península Ibérica mediante el modelo ecológico de nicho MaxEnt. *GeoFocus*, 25, 77–102.
Saponari, M., Giampetruzzi, A., Loconsole, G., Boscia, D. & Saldarelli, P. (2019) *Xylella fastidiosa* in olive in Apulia: where we stand. *Phytopathology*, 109, 175–186.
Schneider, K., der Werf, W., Cendoya, M. & Lansink, A.O. (2020) Impact of *Xylella fastidiosa* subspecies *pauca* in European olives. *Proceedings of the National Academy of Science of the United States of America*, 117, 9250–9259.
Soubeyrand, S., de Jerphanion, P., Martin, O., Saussac, M., Manceau, C., Hendrikx, P. et al. (2018) Inferring pathogen dynamics from temporal count data: the emergence of *Xylella fastidiosa* in France is probably not recent. *New Phytologist*, 219, 824–836.
Thuiller, W., Georges, D., Engler, R. & Breiner, F. (2020) *Package 'biomod2'*. Ensemble Platform species Distribution Modeling. R package version 3.5.1. Available at: https://CRAN.R-project.org/package=biomod2 [Accessed 15 September 2022].
Tumber, K., Alston, J. & Fuller, K. (2014) Pierce's disease costs California $104 million per year. *California Agriculture*, 68, 20–29.
Van Vuuren, D.P., Edmonds, J., Kainuma, M., Riahi, K., Thomson, A., Hibbard, K. et al. (2011) The representative concentration pathways: an overview. *Climate Change*, 109, 5–31.
Watanabe, S., Hajima, T., Sudo, K., Nagashima, T., Takemura, T., Okajima, H. et al. (2011) MIROC-ESM 2010: Model description and basic results of CMIP5-20c3m experiments. *Geoscientific Model Development*, 4, 845–872.
Wells, J.M., Raju, B.C., Hung, H.-Y., Weisburg, W.G., Mandelco-Paul, L. & Brenner, D.J. (1987) *Xylella fastidiosa* gen. nov., sp. nov: gram-negative, xylem-limited, fastidious plant bacteria related to *Xanthomonas* spp. *International Journal of Systemic and Evolutionary Microbiology*, 37, 136–143.

SUPPORTING INFORMATION

Additional supporting information can be found online in the Supporting Information section at the end of this article.

How to cite this article: Godefroid, M., Cruaud, A., Streito, J-C., Rasplus, J-Y. & Rossi, J-P. (2022) Forecasting future range shifts of *Xylella fastidiosa* under climate change. *Plant Pathology*, 00, 1–10. Available from: https://doi.org/10.1111/ppa.13637